Supplementary Material

Please see supplemental figures and tables contained below.

- Figures
  -
  -
  -
  -
  -
  -
  -
  -
  -
  -
- Tables
  -
  -
- Other materials
  - Glossary

Glossary

1. **Atlas abbreviations and definitions**. For further details, see Table. S1.

   (a) **AAL**. Automated anatomical labeling atlas.

   (b) **AAL1, AAL2, AAL3**. AAL atlas versions 1, 2, and 3, respectively.

   (c) **AAL-JHU**. The AAL atlas and the JHU labels atlas combined. For overlapping regions, the JHU atlas takes precedence.

   (d) **AAL600**. AAL atlas with 600 parcels.

   (e) **AICHA**. Atlas of Intrinsic Connectivity of Homotopic Areas.

   (f) **BNA**. Brainnetome atlas.

   (g) **Craddock 200-400**. Craddock atlases with a specified number of parcels (e.g. Craddock 200 will have 200 parcels). There are two atlas sizes publicly available - the Craddock 200 and Craddock 400 atlases.

   (h) **DKT31 OASIS**. The DKT atlas from the OASIS dataset. See Table. S1 sources for more details. It is the volumetric version.

   (i) **DKT40**. The DKT atlas used as part of FreeSurfer. See Table. S1 sources for more details. It is the surface version.

   (j) **DK**. The Desikan-Killiany atlas. Surface atlas from FreeSurfer.

   (k) **HO**. Harvard-Oxford atlas.

   (l) **HO cortical-only**. HO atlas with only cortical regions. The symmetrical regions (the same region name on the contralateral hemisphere) are labeled with *different* identifications. Thus, this atlas has *non-symmetrical* labels (e.g. both temporal pole regions are labeled with a different identification number). Left and right structures were re-labeled with different identification numbers using the sagittal mid-line (in MNI space, x coordinate at zero) as a separator.

   (m) **HO cort-only**. Same as the HO cortical-only atlas.

   (n) **HO sym. cortical only**. HO atlas with only cortical regions. The symmetrical regions (the same region name on the contralateral hemisphere) are labeled with the *same* identification. Thus, this atlas is has *symmetrical* labels (e.g. both temporal pole regions are labeled with the same identification number). The default atlases given by FSL are symmetrical atlases.

   (o) **HO subcortical-only**. HO atlas with only subcortical regions.

   (p) **HO subcort-only**. Same as the HO subcortical-only atlas.

   (q) **HO combined**. HO atlas with both cortical and subcortical regions. This atlas has non-symmetrical labeling (e.g. both temporal pole regions are labeled with a different identification number).

   (r) **HO cortical + subcortical**. Same as the HO combined atlas.

   (s) **JHU**. The Johns Hopkins University atlases. There are two white matter atlases: thee JHU labels and JHU tracts atlases.

   (t) **MMP**. Multi-modal parcellation atlas. Sometimes referred to as the "Glasser Atlas" after the first author of the original publication.

   (u) **Random atlas 10-10,000**. Atlases created with random parcels with a specified number of parcels (e.g. Random atlas 1,000 will have 1,000 parcels). These atlases were built in the ICBM 2009c Nonlinear Asymmetric template. Thus, these atlases are whole-brain atlases (includes cortical gray matter, subcortical gray matter, and white matter). See the 'Atlases' Methods section for more details.

   (v) **Schaefer 100-1,000**. The Schaefer atlases with a specified number of parcels (e.g. Schaefer 100 will have 100 parcels). There are ten atlases of 100, 200, 300, 400, 500, 600, 700, 800, 900, and 1,000 parcels.

   (w) **Yeo liberal**. The Yeo atlases where the boundaries of each parcel is extended slightly into the white matter, past the cortical boundary.

   (x) **Yeo conservative**. The Yeo atlases where the boundaries of each parcel is extended slightly into the white matter, past the cortical boundary.

2. Δ **SFC**. The change in SFC between ictal and preictal stats ($SFC_{ictal} - SFC_{preictal}$). This indicates whether or not the change in functional connectivity is congruent with the underlying structural connectivity.

3. **Contact**. A single sensor on an electrode that records LFP. Not to be confused with an electrode. See Fig. S7, bottom.

4. **ECoG**: Electrocorticography.

5. **Electrode**. Not to be confused with contact. See Fig. S7, bottom.

6. **Derived atlas**: An atlas which was derived from another atlas. For example, the AAL 600 is derived from the AAL atlas in which its parcellations are further sub-divided using a specified algorithm. Derived atlases may also be sub-divided randomly so that it is both considered a random and derived atlas (a quasi-random atlas). The BNA is also a derived atlas in which it initially used the parcellations of the DK atlas.

7. **Functional connectivity (FC)**. The statistical relationship between two signals (two contacts in this study).

8. **grayordinate**. Atlas that includes gray matter structures, including cortical and subcortical gray matter regions.

9. **ROI**. Region of interest

10. **ROI, parcel, parcellation, region**. These terms may be used interchangeably in the literature. They refer to discrete areas of a brain. These regions are labeled with a categorical identification (rather than a continuous variable seen in templates - see Fig. S1), and all voxels or surface vertices with the same identification are part of thee same region.

11. **SEEG**: Stereoelectroeenccephalography.

12. **Structural connectivity (SC)**. The physical relationship between two brain regions. We use streamline counts in this manuscript from High Angular Resolution Diffusion Imaging.

13. **T1w**. T1-weighted MRI image.

Clarifying Terminologies

a **Atlas**

b **Template**
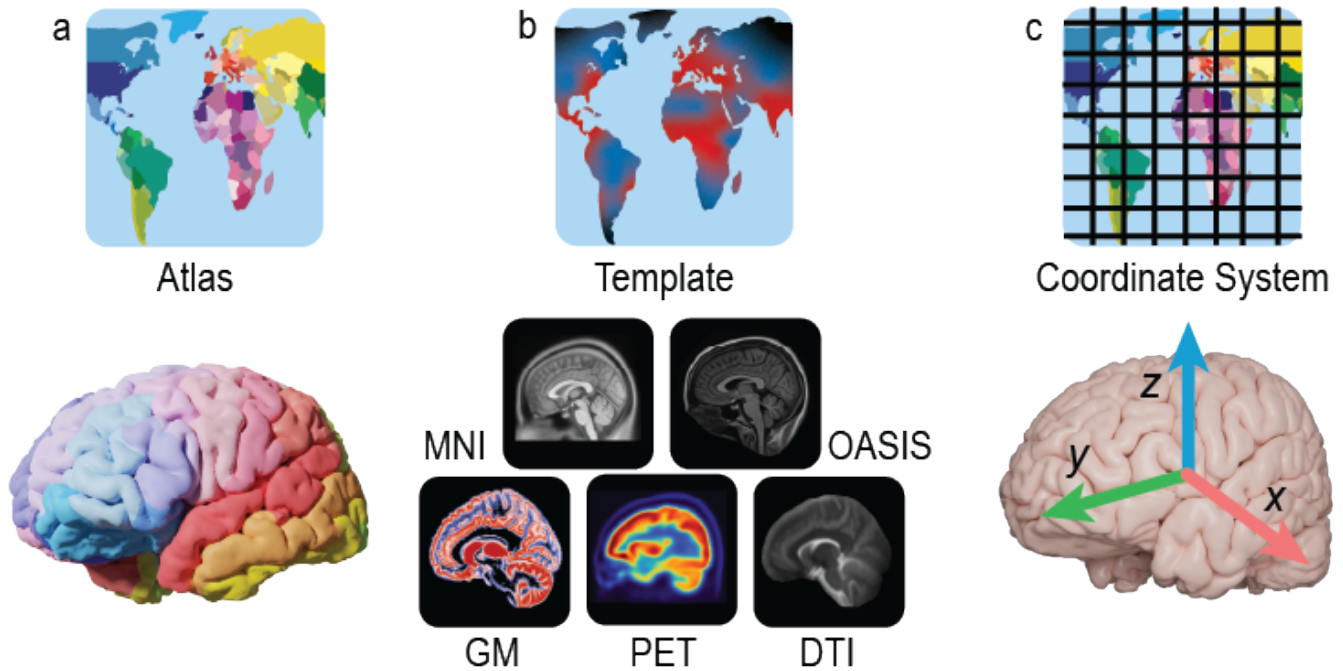
MNI OASIS

GM PET DTI

c **Coordinate System**

Fig. S1. Atlas, Template, and Coordinate (Stereotactic) Space. | These three terms are commonly confused in the neuroscience literature because they all relate to the "map" of the brain. "Atlas" and "template" are sometimes used interchangeably[3], however, they are distinct. Here, we define them more formally. **a**, A brain ***atlas*** refers to a neurological map that defines brain region *labels*. We use this definition throughout the main text. **b**, An atlas is distinct from a brain ***template***, which refers to a brain *pattern*. Similar in common usage, a template is a mold, gauge, or starting point representation of the brain. Usually it is composed of multiple individuals' brain representing an average of a population. Many templates exist and are reviewed in various publications[2,9], The templates illustrated here are the MNI152 Nonlinear asymmetric 2009c T1w template (http://www.bic.mni.mcgill.ca), the OASIS brain template https://www.oasis-brains.org/ created and used by ANTs (http://stnava.github.io/ANTs/ with templates linked here), a gray matter probability map, a PET template, and a b0 DTI template. **c**, The coordinate system, or the **stereotactic space**, of the brain describes the physical positioning of the brain, similar to the geographical coordinate system of longitude and latitude of the Earth. Historically, a common stereotactic space was the Talairach space, and more recently, the MNI spaces. The analogy between the geographical terms of the Earth and the geographical terms of the brain is not exact. The analogy falls apart in that while there in one world, there are many brains. There is variability across populations and a spectrum of differences between species, therefore, it is challenging to represent one brain for use in every scientific study appropriately. **MNI**, Montreal Neurological Institute; **OASIS**, Open Access Series of Imaging Studies; **GM**, Gray Matter probability map; **PET**, Positron Emission Tomography; **DTI**, Diffusion Tensor Imaging.
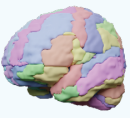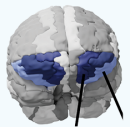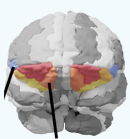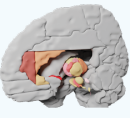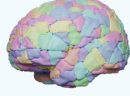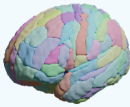
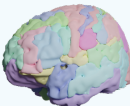| Atlas	Source	Note	Reference(s)
AAL	1	AAL1. The successor to the Talairach atlas. The goal was to reduce confusion in relating stereotaxic space (a set of brain coordinates) and anatomical labels. It is based on a single individual (the Collin-27 template) and it is not a probabilistic map. The Collin-27 template was intended for segmentation, and not stereotaxy; it did not capture anatomical variability. However, the high resolution in 1998 proved attractive to research groups.	(1) Tzourio-Mazoyer, N. et al. Automated Anatomical Labeling of Activations in SPM Using a Macroscopic Anatomical Parcellation of the MNI MRI Single-Subject Brain. NeuroImage 15, 273–289 (2002). (2) Collin-27 template: Holmes, C. J. et al. Enhancement of MR Images Using Registration for Signal Averaging: Journal of Computer Assisted Tomography 22, 324–333 (1998). (3) Website about Collin-27: https://www.bic.mni.mcgill.ca/ServicesAtlases/Colin27
	2	AAL2: new parcellation of orbitofrontal cortex. AAL1 orbitofrontal cortex was parcellated according to a French publication by Jules Déjerine in 1895. Chiavaras and Petrides (2000) proposed another parcellation of the orbital surface allowing for the comparison of human frontal lobe anatomy with that of macaques.	(1) Rolls, E. T., Joliot, M. & Tzourio-Mazoyer, N. Implementation of a new parcellation of the orbitofrontal cortex in the automated anatomical labeling atlas. NeuroImage 122, 1–5 (2015). (2) Chiavaras, M. M. & Petrides, M. Orbitofrontal sulci of the human and macaque monkey brain. The Journal of Comparative Neurology 422, 35–54 (3) Dejerine, J. Anatomie des centres nerveux. (Rueff Paris, 1895).
	3	AAL3: new parcellations - anterior cingulate, thalamus, nucleus accumbens, substantia nigra, ventral tegmental area, red nucleus, locus coeruleus, and raphe nuclei. 2019. AAL3v1: changes of thalamus in line with FreeSurfer 7. 2020.	Rolls, E. T., Huang, C.-C., Lin, C.-P., Feng, J. & Joliot, M. Automated anatomical labelling atlas 3. NeuroImage 206, 116189 (2020).
	4	Website for download - group that made AAL toolbox and user guides.	https://www.gin.cnrs.fr/en/tools/aal/
	5	SPM - software compatible with AAL toolbox. Generally, designed for the analysis of brain imaging data sequences. Extensions include AAL toolbox.	(1) Statistical parametric mapping: the analysis of functional brain images. (Elsevier/Academic Press, 2007). (2) Website: https://www.fil.ion.ucl.ac.uk/spm/ext/
	6	AAL 600 - Subparcellations of the AAL atlas into 600 subregions. Upsampling algorithm described. Part of larger framework for evaluating the effect of parcellation scale.	Bassett, D. S., Brown, J. A., Deshpande, V., Carlson, J. M. & Grafton, S. T. Conserved and variable architecture of human white matter connectivity. NeuroImage 54, 1262–1279 (2011)
	7	Use cases of AAL600. Both Ashourvan et al. (2017) and Hermundstad et al. (2014) use AAL600 for generating both structural and functional connectivity networks.	(1) Ashourvan, A., Telesford, Q. K., Verstynen, T., Vettel, J. M. & Bassett, D. S. Multiscale detection of hierarchical community architecture in structural and functional brain networks. (2017) (2) Hermundstad, A. M. et al. Structurally-Constrained Relationships between Cognitive States in the Human Brain. PLoS Comput Biol 10, e1003591 (2014).
AICHA	8	AICHA tries to account for *homotopy*: the concept that each region in one hemisphere has a homologue in the other.	Joliot, M. et al. AICHA: An atlas of intrinsic connectivity of homotopic areas. Journal of Neuroscience Methods 254, 46–59 (2015)
Brainnetome	9	Connectivity-based atlas. Further subdivision of structural parcellations using the DK (Desikan-Killiany) protocol, with adjustments.	Fan, L. et al. The Human Brainnetome Atlas: A New Brain Atlas Based on Connectional Architecture. Cerebral cortex (New York, N.Y. : 1991) 26, 3508–26 (2016). Website: http://atlas.brainnetome.org
	10	DSI studio created by Fang-Cheng (Frank) Yeh. Many reconstruction and tracking algorithms are published and incorporated into DSI Studio. See citations page on website. Many atlases available, including Brainnetome. Can use custom atlas.	(1) Website: http://dsi-studio.labsolver.org/ (2) Example of reconstruction method: Fang-Cheng Yeh, Wedeen, V. J. & Tseng, W.-Y. I. Generalized q-Sampling Imaging. IEEE Trans. Med. Imaging 29, 1626–1635 (2010).
Brodmann	11	Perspective, description, and historical significance of Korbinian Brodman's map.	Zilles, K. & Amunts, K. Centenary of Brodmann's map — conception and fate. Nat Rev Neurosci 11, 139–145 (2010
	12	References to the original German and English translation provided.	(1) Original German: Vergleichende Lokalisationslehre der Grosshirnrinde in ihren Prinzipien dargestellt auf Grund des Zellenbaues. (1909) (2) English translation: Brodmann, K. & Gary, L. J. Brodmann's localisation in the cerebral cortex: the principles of comparative localisation in the cerebral cortex based on cytoarchitectonics. (Springer, 2006
	13	The atlas is available through MRIcro, a legacy tool developed by Chris Rorden (University of South Carolina). The atlas is based on work from the Van Essen lab (Washington University in St. Louis) with corresponding Talairach coordinates, and transformed by Krish Singh (Cardiff University) to MNI space.	(1) Chris Rorden legacy tools webpage: https://people.cas.sc.edu/rorden/ (2) Updated webpage: https://crnl.readthedocs.io/ (3) About Brodmann atlas: https://people.cas.sc.edu/rorden/mricro/lesion.html (4) BALSA: https://balsa.wustl.edu/Wz8r
CerebrA	14	Introduction to the CerebrA and MNI-ICBM2009c average brain template.	Manera, A. L., Dadar, M., Fonov, V. & Collins, D. L. CerebrA, registration and manual label correction of Mindboggle-101 atlas for MNI-ICBM152 template. Sci Data 7, 237 (2020). Website: https://doi.gin.g-node.org/10.12751/g-node.be5e62
Craddock	15	Original publication about functional parcellations.	Craddock, R. C., James, G. A., Holtzheimer, P. E., Hu, X. P. & Mayberg, H. S. A whole brain fMRI atlas generated via spatially constrained spectral clustering. Hum. Brain Mapp. 33, 1914–1928 (2012).
	16	GitHub with source code to make atlas with N clusters.	GitHub: http://ccraddock.github.io/cluster_roi/atlases.html
	17	Publicly available pre-made atlases at N=200 and N=400 from ABIDE (Autism Brain Imaging Data Exchange), co-founded by Cameron Craddock. 4x4x4mm resolution.	ABIDE: http://preprocessed-connectomes-project.org/abide/Pipelines.html

Table S1. Atlas sources and references. | This table provides a short note and references to the source material of common atlases in the neuroscience literature. See also Table 1.
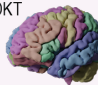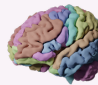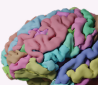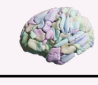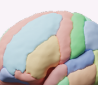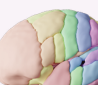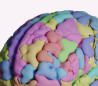
Atlas	Source	Note	Reference(s)
DKT Surface version Volumetric version DK atlas - surface (original DK protocol)	18	Original DK protocol and atlas. A protocol for an atlas is a set of instructions for how the brain should be labeled. See AAL, Hammersmith, Harvard-Oxford, and JHU atlases.	Desikan, R. S. et al. An automated labeling system for subdividing the human cerebral cortex on MRI scans into gyral based regions of interest. NeuroImage 31, 968–980 (2006).
	19	DKT protocol, Mindboggle-101 dataset, and atlas creation.	Klein, A. & Tourville, J. 101 Labeled Brain Images and a Consistent Human Cortical Labeling Protocol. Front. Neurosci. 6, (2012).
	20	Summary of Mindboggle project, history, atlas development, applications, and current problems.	Klein, A. et al. Mindboggling morphometry of human brains. PLoS Comput Biol 13, e1005350 (2017)
	21	Websites for downloading data including the labeled brains and atlases.	Open Science Framework: https://osf.io/nhtur/ Harvard Dataverse: https://dataverse.harvard.edu/dataverse/mindboggle Labels: https://mindboggle.readthedocs.io/en/latest/labels.html GitHub: https://github.com/nipy/mindboggle
	22	Subcortical regions.	http://www.neuromorphometrics.com/
	23	FreeSurfer.	https://surfer.nmr.mgh.harvard.edu/
Destrieux	24	Original article describes automatic labeling algorithm from probabilistic information using a manually labeled training set. 74 parcellations per hemisphere (excluding subcortical structures). Available in FreeSurfer with subcortical structures output.	(1) Destrieux, C., et al., E. Automatic parcellation of human cortical gyri and sulci using standard anatomical nomenclature. NeuroImage 53, 1–15 (2010). (2) Fischl, B. Automatically Parcellating the Human Cerebral Cortex. Cerebral Cortex 14, 11–22 (2004).
	25	FreeSurfer information on atlases available.	(1) https://surfer.nmr.mgh.harvard.edu/fswiki/CorticalParcellation (2) https://surfer.nmr.mgh.harvard.edu/fswiki/DestrieuxAtlasChanges
Gordon-Petersen	26	Original article.	Gordon, E. M. et al. Generation and Evaluation of a Cortical Area Parcellation from Resting-State Correlations. Cereb. Cortex 26, 288–303 (2016).
	27	Resource to download atlas.	https://sites.wustl.edu/petersenschlaggarlab/resources/
Hammersmith	28	Original article (for regions 1-49), including their Hammersmith protocol (or "algorithm").	Hammers, A. et al. Three-dimensional maximum probability atlas of the human brain, with particular reference to the temporal lobe. Hum. Brain Mapp. 19, 224–247 (2003).
	29	Updated regions (for regions 50-83).	Gousias, I. S. et al. Automatic segmentation of brain MRIs of 2-year-olds into 83 regions of interest. NeuroImage 40, 672–684 (2008).
	30	Download atlas with 83 regions.	http://brain-development.org/brain-atlases/adult-brain-atlases/adult-brain-maximum-probability-map-hammers-mith-atlas-n30r83-in-mni-space/
Harvard-Oxford	31	Atlas developed at the Center for Morphometric Analysis (CMA) at Massachusetts General Hospital and distributed with FSL.	https://fsl.fmrib.ox.ac.uk/fsl/fslwiki/Atlases
	32	Individual segmentations were segmented by CMA using in-house software. Probability maps were then created. Freesurfer link (right) has archived CMA's website and contains the Harvard-Oxford labeling protocols.	FreeSurfer description about CMA: http://freesurfer.net/fswiki/CMA Link to website archive: https://web.archive.org/web/20180413052010/http://www.cma.mgh.harvard.edu/
JHU	33	JHU labels: Protocol to reconstruct eleven white matter tracts and their segmentation into ROI labels. Included in FSL.	Wakana, S. et al. Reproducibility of quantitative tractography methods applied to cerebral white matter. NeuroImage 36, 630–644 (2007).
	34	JHU Tracts: white matter parcellation atlas based on DTI probabilistic tractography of 11 major white matter tracts d. Protocol defining manually identified ROIs from which the tracts were formed are described in Wakana et al. (2005). Included in FSL.	Hua, K. et al. Tract probability maps in stereotaxic spaces: Analyses of white matter anatomy and tract-specific quantification. NeuroImage 39, 336–347 (2008).
	35	Textbook with more information about these atlases.	MRI atlas of human white matter. (Elsevier, Acad. Press, 2011).
Julich	36	Cytoarchitecture map. Successor to both the Brodmann and Eickhoff-Zilles atlases. The Eichoff-Zilles is an SPM toolbox (see note is source 5 about the AAL atlas) for probabilistic cytoarchitecture.	(1) Amunts, K., Mohlberg, H., Bludau, S. & Zilles, K. Julich-Brain: A 3D probabilistic atlas of the human brain's cytoarchitecture. 6 (2020). (2) Eickhoff, S. B. et al. A new SPM toolbox for combining probabilistic cytoarchitectonic maps and functional imaging data. NeuroImage 25, 1325–1335 (2005)
	37	Website for the Julich Atlas and SPM toolbox.	https://www.fz-juelich.de/inm/inm-1/DE/Forschung/_docs/SPMAnatomyToolbox/SPMAnatomyToolbox_node.html
MMP	38	Original article on multi-modal approach.	Glasser, M. F. et al. A multi-modal parcellation of human cerebral cortex. Nature 536, 171–178 (2016).
	39	Information on surface vs volume based methodologies for localization of neuroanatomy.	Coalson, T. S., Van Essen, D. C. & Glasser, M. F. The impact of traditional neuroimaging methods on the spatial localization of cortical areas. Proc Natl Acad Sci USA 115, E6356–E6365 (2018).
	40	Website to download data. Volumetric version also included in DSI-studio. Note the volume note above.	https://balsa.wustl.edu/

Table S1. (cont.) Atlas sources and references. | This table provides a short note and references to the source material of common atlases in the neuroscience literature. See also Table 1.

Atlas	Source	Note	Reference(s)
Random	41	Random atlas algorithm (pseudo-grassfire algorithm).	Zalesky, A. et al. Whole-brain anatomical networks: does the choice of nodes matter? Neuroimage 50, 970–83 (2010).
	42	Use case of random atlas. Goni et al. (2014) study the structure-function relationship in the brain with tractography and fMRI. They used random cortical atlases of 1170 equally sized regions. Misic et al. (2015) used random cortical atlases of 1015 equally sized regions.	(1) Goni, J. et al. Resting-brain functional connectivity predicted by analytic measures of network communication. Proceedings of the National Academy of Sciences 111, 833–838 (2014). (2) Mišić, B. et al. Cooperative and Competitive Spreading Dynamics on the Human Connectome. Neuron 86, 1518–29 (2015).
MNI Structural	43	Included with FSL. See website for further details. Included structures are (1) Caudate, (2) Putamen, (3) Thalamus, (4) Insula, (5) Frontal lobe, (6) Temporal lobe, (7) Parietal lobe, (8) Occipital lobe, and (9) Cerebellum.	(1) Website: http://www.talairach.org/about.html (2) http://www.talairach.org/about.html (3) Mazziotta, J. et al. A probabilistic atlas and reference system for the human brain: International Consortium for Brain Mapping (ICBM). Phil. Trans. R. Soc. Lond. B 356, 1293–1322 (2001).
Schaefer	44	Original publication about functional parcellations.	Schaefer, A. et al. Local-Global Parcellation of the Human Cerebral Cortex from Intrinsic Functional Connectivity MRI. Cerebral Cortex 28, 3095–3114 (2018).
	45	GitHub and detailed documentation of atlases.	https://github.com/ThomasYeoLab/CBIG/tree/master/stable_projects/brain_parcellation/Schaefer2018_LocalGlobal
Talairach	46	Download: Included with FSL. Also available through website.	Website: http://www.talairach.org/
	47	The anatomical region labels were electronically derived from axial sectional images in the 1988 Talairach Atlas. The atlas was digitized and manually traced into a volume-occupant hierarchy of anatomical regions detailed these publications (i.e. the pages of the 1988 textbook with drawings were photocopied and transformed into the computerized coordinate system).	(1) Lancaster, J. L., Evans, A. C. & Toga, A. W. Automated Labeling of the Human Brain: A Preliminary Report on the Development and Evaluation of a Forward-Transform Method. 238–242 (1997). (2) Lancaster, J. L. et al. Automated Talairach Atlas Labels For Functional Brain Mapping. 120–131 (2000).
	48	(1) First atlas in 1957 focusing on the subcortical deep gray nucelli, (2) second atlas in 1967 focusing on the telencephalon, (3) third atlas in 1988 focusing on the whole brain. Most researchers preferred the use of the Talairach atlas to report the localization of the activations detected in functional imaging studies because it offers a detailed anatomical brain description within the stereotaxic space, including Brodmann's areas.	(1) Talairach, J., David, M., Tournoux, P., Corredor, H. & Kvasina, T. Atlas d'Anatomie Stéréotaxique. Repérage Radiologique Indirect des Noyaux Gris Centraux des Régions Mésencephalosousoptique et Hypothalamique de l'Homme. (1957). (2) Talairach, J. & Szikla, G. Atlas of Stereotaxic Anatomy of the Telencephalon. (Masson, 1967) (3) Talairach, J. & Tournoux, P. Co-planar stereotaxic atlas of the human brain: 3-dimensional proportional system: an approach to cerebral imaging. (Georg Thieme, 1988).
	49	Historical publication about Jean Talairach.	Harary, M. & Cosgrove, G. R. Jean Talairach: a cerebral cartographer. Neurosurgical Focus 47, E12 (2019).
	50	Comparison between MNI and Talairach Coordinates.	Lancaster, J. L. et al. Bias between MNI and Talairach coordinates analyzed using the ICBM-152 brain template. Hum. Brain Mapp. 28, 1194–1205 (2007).
Yeo	51	Original publication about functional parcellations.	Thomas Yeo, B. T. et al. The organization of the human cerebral cortex estimated by intrinsic functional connectivity. Journal of Neurophysiology 106, 1125–1165 (2011)
	52	Website from FreeSurfer.	https://surfer.nmr.mgh.harvard.edu/fswiki/CorticalParcellation_Yeo2011
Region-specific	53	Thalamus - based on ex vivo analysis.	Iglesias, J. E. et al. A probabilistic atlas of the human thalamic nuclei combining ex vivo MRI and histology. NeuroImage 183, 314–326 (2018).
	54	Hippocampus - based on ex vivo analysis.	Iglesias, J. E. et al. A computational atlas of the hippocampal formation using ex vivo, ultra-high resolution MRI: Application to adaptive segmentation of in vivo MRI. NeuroImage 115, 117–137 (2015).
	55	Structural atlas of Cerebellum. Included with FSL.	Diedrichsen, J., Balsters, J. H., Flavell, J., Cussans, E. & Ramnani, N. A probabilistic MR atlas of the human cerebellum. NeuroImage 46, 39–46 (2009).
	56	Functional atlas of Cerebellum.	(1) Xue, A. et al. The Detailed Organization of the Human Cerebellum Estimated by Intrinsic Functional Connectivity Within the Individual. 69. (2) Buckner, R. L., Krienen, F. M., Castellanos, A., Diaz, J. C. & Yeo, B. T. T. The organization of the human cerebellum estimated by intrinsic functional connectivity. Journal of Neurophysiology 106, 2322–2345 (2011). (2) GitHub: https://github.com/ThomasYeoLab/CBIG/tree/master/stable_projects/brain_parcellation/Xue2021_IndCerebellum
Population-specific	57	Pediatric/Neonatal.	Alexander, B. et al. A new neonatal cortical and subcortical brain atlas: the Melbourne Children's Regional Infant Brain (M-CRIB) atlas. NeuroImage 147, 841–851 (2017).
	58	Disease-specific: example of a multiple sclerosis lesional atlas.	Sahraian, M. A. & Radue, E.-W. MRI atlas of MS lesions. (Springer, 2008).

Table S1. (cont.) Atlas sources and references. | This table provides a short note and references to the source material of common atlases in the neuroscience literature. See also Table 1.
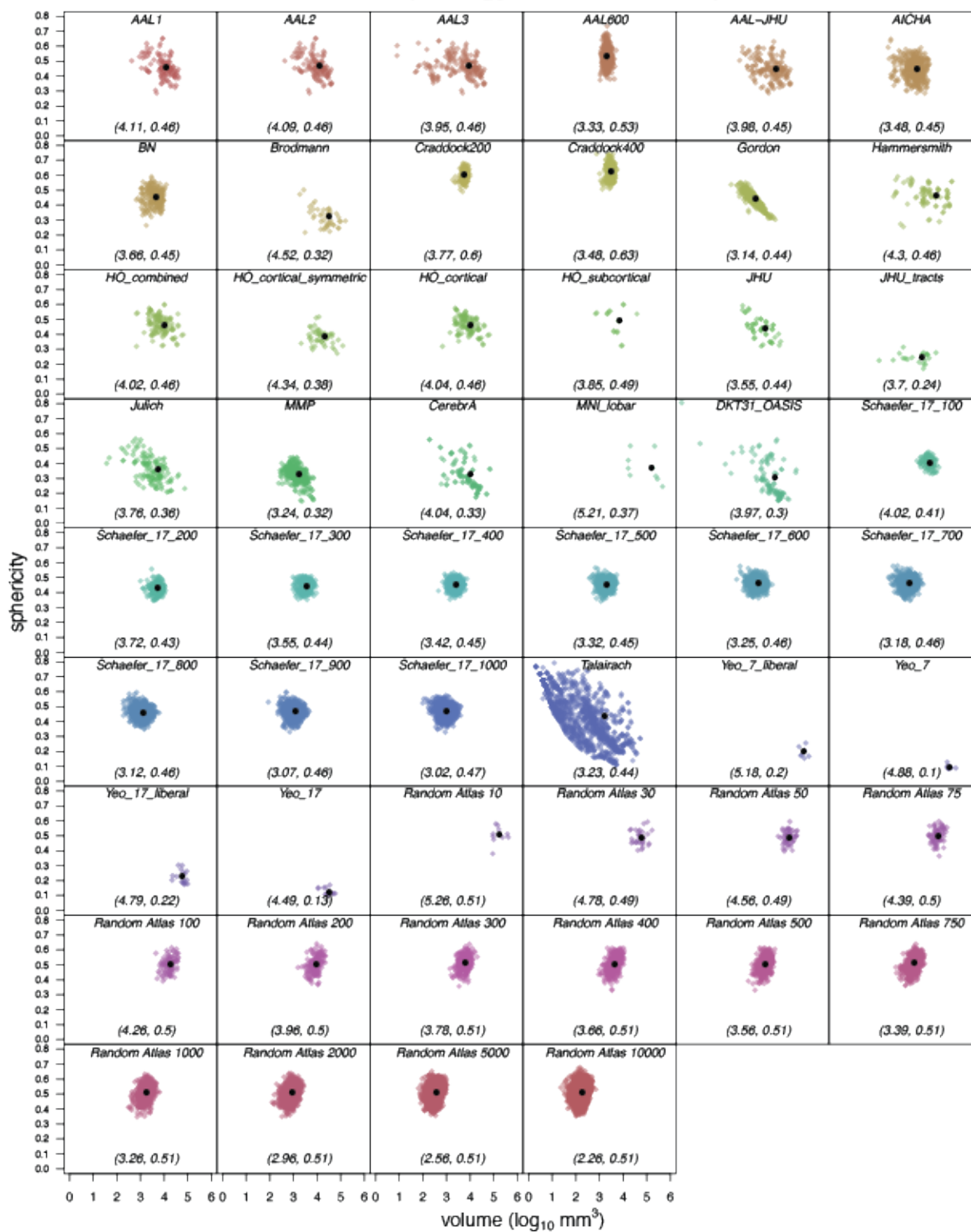
Fig. S2. Atlas Morphology: Sizes and Shapes. | All standard atlases and one permutation for each of the standard atlases are shown here. Volume means and sphericity means are in parentheses at the bottom of each graph. See Table S1 for atlas abbreviations, descriptions, and sources.
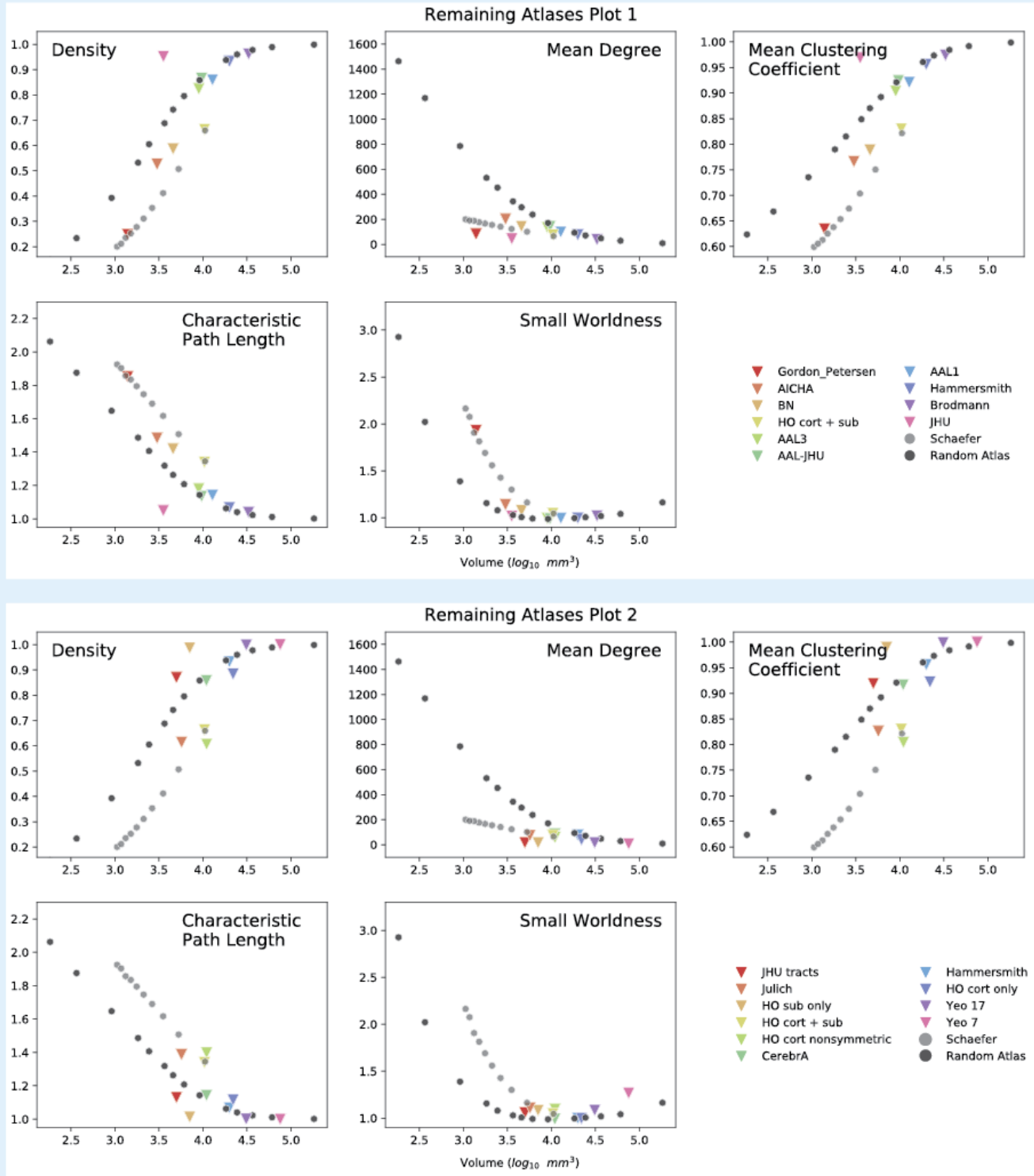
Fig. S3. Structure-Function Correlation (SFC) for All Atlases. | We show network measures the remaining atlases illustrated in Table 2. See Table S1 for atlas descriptions. **HO**, Harvard-Oxford; **Sub**, subcortical; **Cort**, cortical
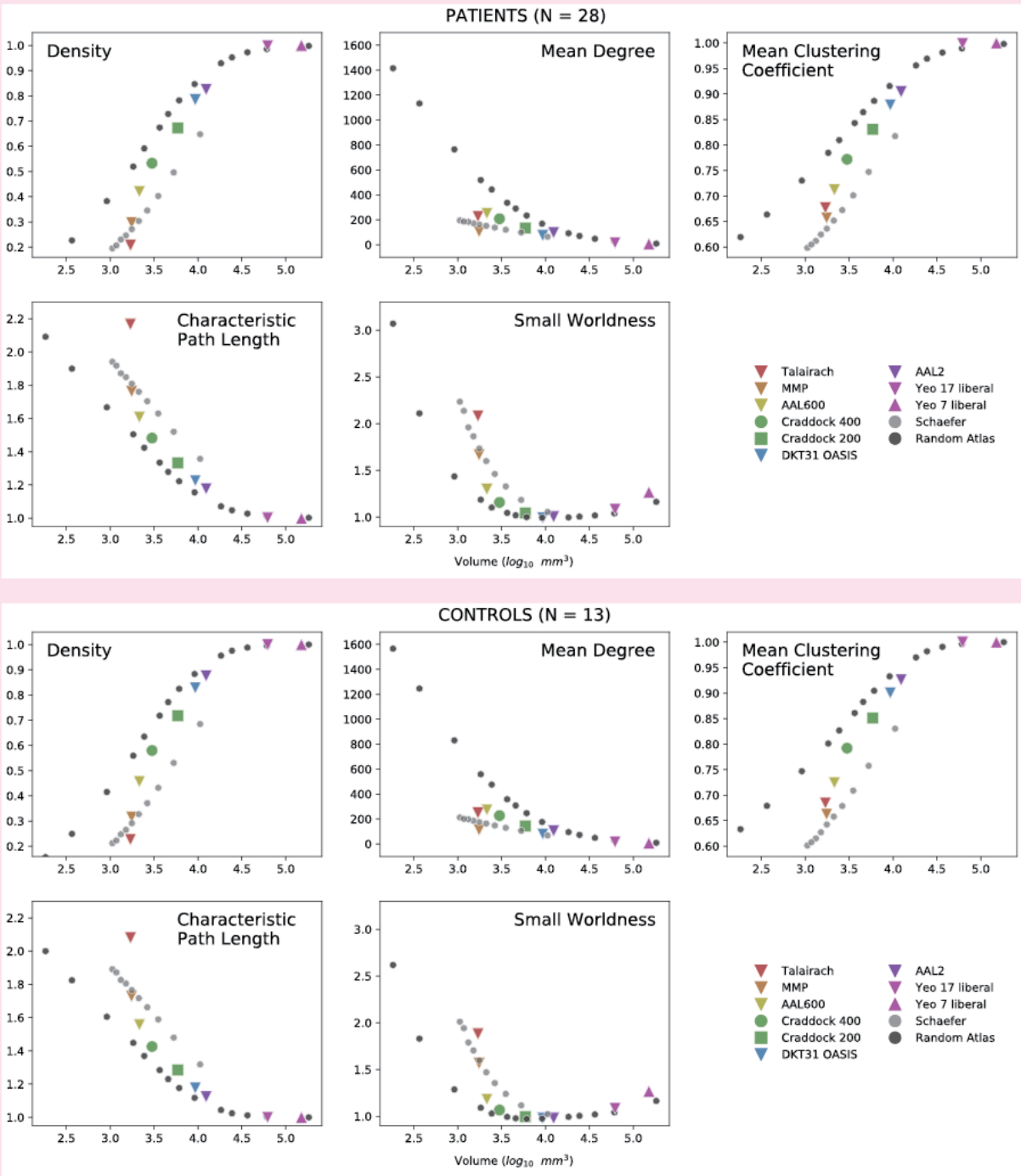
Fig. S4. Network Measures: Controls vs Patients. | We replicate Fig. 2 (N=41) in the manuscript by separating out controls (N=13) and patients (N=28). All global network measures above are similar between patients and controls, with patients having slightly lower (but not significant, Fig. 2 bottom right panel) measurements for the different network properties. Specific connectivity differences between controls and patients were not explored (e.g. to explore if connections from the hippocampus to the anterior cingulate are changed in temporal lobe epilepsy) and out of the scope of this manuscript. See Table S1 for atlas descriptions.

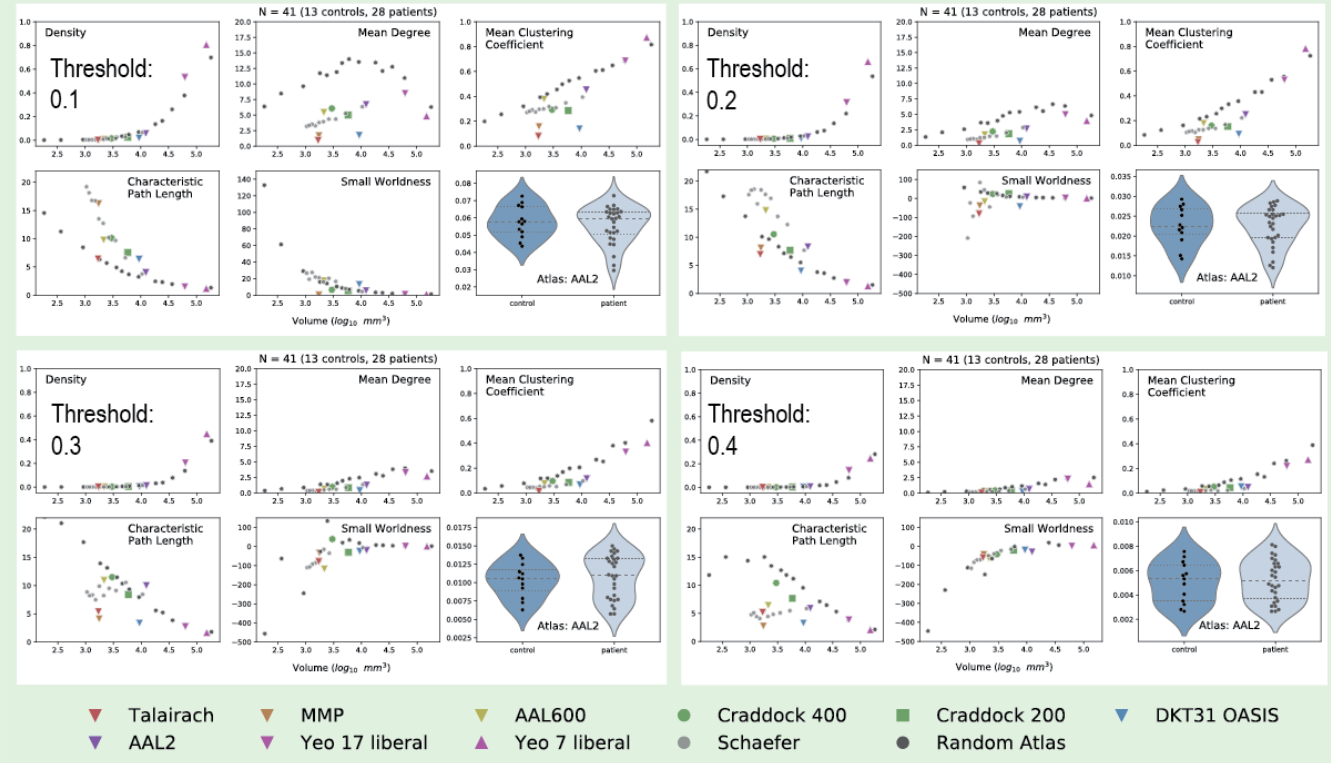**Fig. S5. Network Measures: different thresholds.** | We replicate Fig. 2 (N=41) in the manuscript by calculating network measures using different thresholds. The main text figure includes all weights with no threshold (threshold = 0). We set thresholds at 01., 0.2, 0.3, and 0.4. This was done to show how various network measures may also change when eliminating low-level connections at different thresholds.
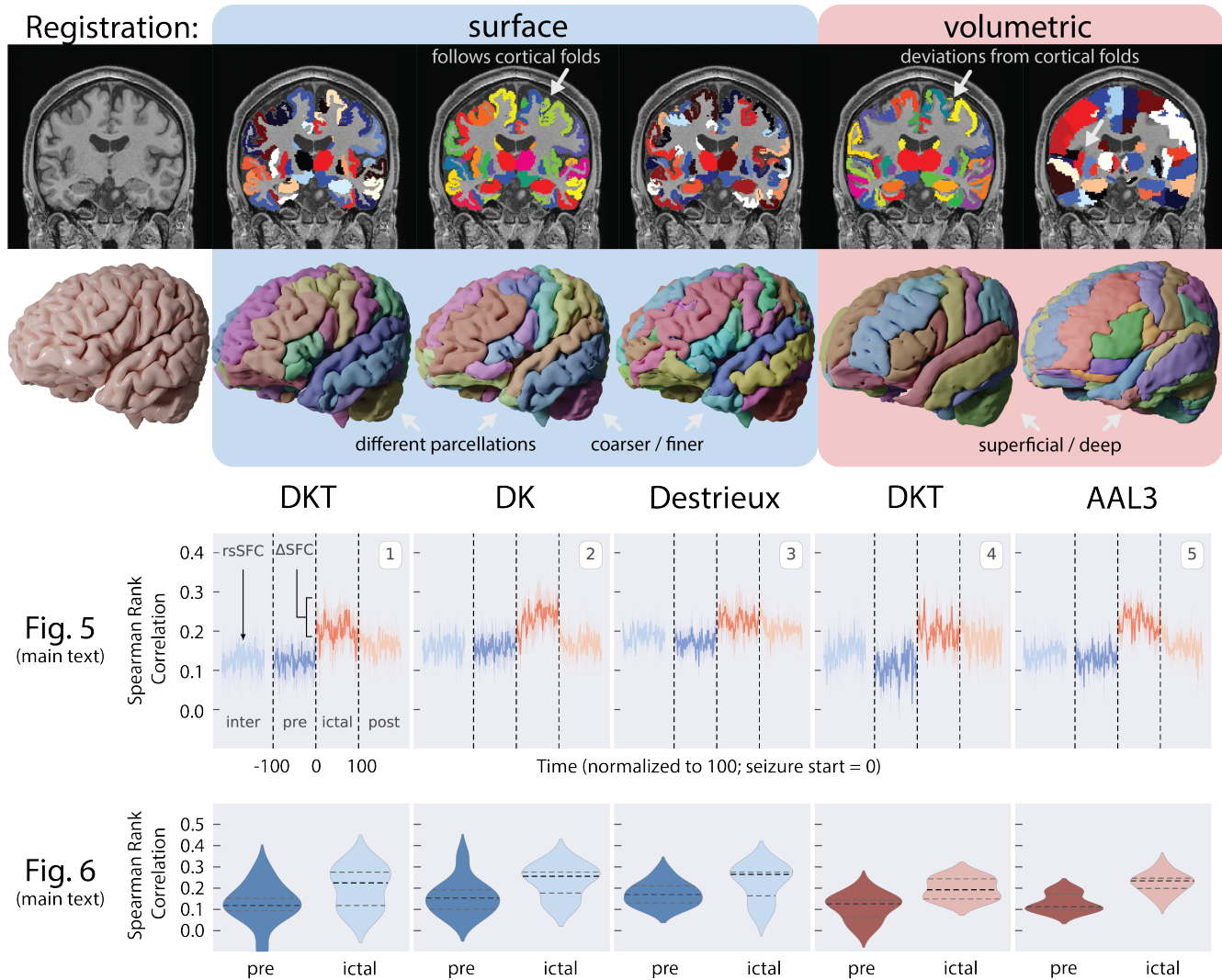
Fig. S6. Effects of Registration: Volumetric- and Surface-based approaches | Volumetric-based analyses, as opposed to surface-based analyses, have been more prevalent in human neuroimaging studies for the last few decades[21]. Volumetric-based approaches to map the neocortex have been shown to be inaccurate in some cases. For example, the top row shows a single subject's T1w image and the resulting labels of three atlases registered using a surface-based approach and two atlases using a volumetric-based approach. The DKT atlas using a surface-based approach follows the cortical folds of the T1w image closely, but the DKT atlas registered using a volumetric-based approach may have many mis-aligned areas. These images show the improved accuracy in mapping and labeling brain structures using surface-based analyses, but the adoption of surface-based analyses has been slow and attributed to five main reasons discussed in Coalson et. al 2018[21]. Briefly, it is due to (1) the need to compare results with existing volumetric-based studies, (2) the prevalence of volumetric-based tools compared to surface-based tools, (3) the learning curve of surface-based approaches; (4) an unawareness of the problems and benefits of each approach; (5) and uncertainty or skepticism as to how much of a difference these methodological choices make. In some cases, it may make a difference, however, it does not make a difference in this study. Here, we used a surface-based approach to register three different atlases to each patient. The atlases were outputs of FreeSurfer's recon-all pipeline[78] - the DKT40, Desikan-Killiany (DK), and Destrieux atlases. The DKT atlas has a modified parcellations of the DK atlas, and the Destrieux atlas is an alternative atlas offered by the FreeSurfer piepline. The Destrieux atlas has a finer parcellation scheme (i.e., more number of regions). We repeat analyses of Fig. 5 and Fig. 6 of the main text, along with results from two volumetric-based atlases for side-by-side comparison. The volumetric-based atlases include the DKT (DKT31 OASIS) and AAL3 atlases. While the volumetric DKT atlas does not properly align and label the entire cortical gray matter regions, the AAL atlas extends deeply into the white matter and does label much of these gray matter regions. For the experimental design of this study in localizing electrode contacts and measuring structural connectivity, the AAL3 atlas provides the most power out of all these atlases in detecting a change in SFC. In the original AAL manuscript[88], the authors "chose to extend the internal limit of the regions beyond the gray matter layer [to account for] anatomical variability". This extension past the internal gray matter boundary may be optimal in our case for measuring SFC because the parcellations may capture streamlines that otherwise would have ended prematurely before reaching gray matter.
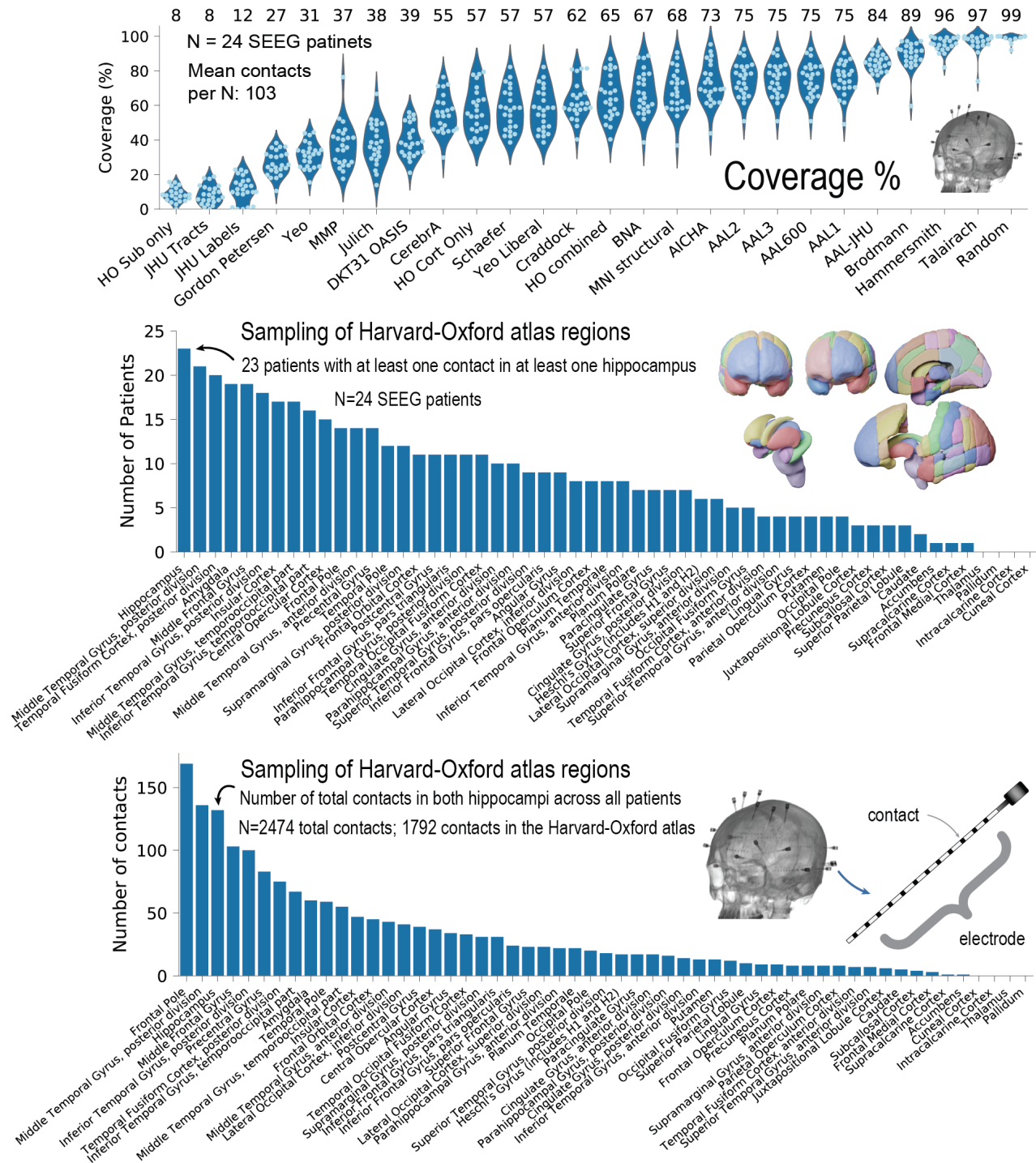
Fig. S7. Coverage of electrode contacts. | Top: We show the percentage of contacts assigned a region given an atlas. If a contact fell outside an atlas, it would not be assigned a location and would not be used in SFC analysis. We also show the Harvard-Oxford atlas regions (cortical and subcortical combined) that contain electrode contacts (middle and bottom figures). The middle figure shows the number of patients with at least one contact in an atlas region (at least one of the regions on both hemispheres). The bottom figure shows the total number of contacts in each listed region. Note that 1792 out of 2474 contacts (72%) contained within the brain parenchyma (gray matter or white matter) is higher than the mean percent coverage listed in the top figure (65% for the HO combined) because some patients with fewer contacts may have lower coverage by the atlas, thus bringing the mean percent down. Also note the larger number of contacts in the frontal pole because this region in the Harvard-Oxford atlas is large. We chose to show the Harvard-Oxford atlas because it has the largest effect size in Fig. 6.

Results for "Brain Atlas" per 100,000 citations in PubMed
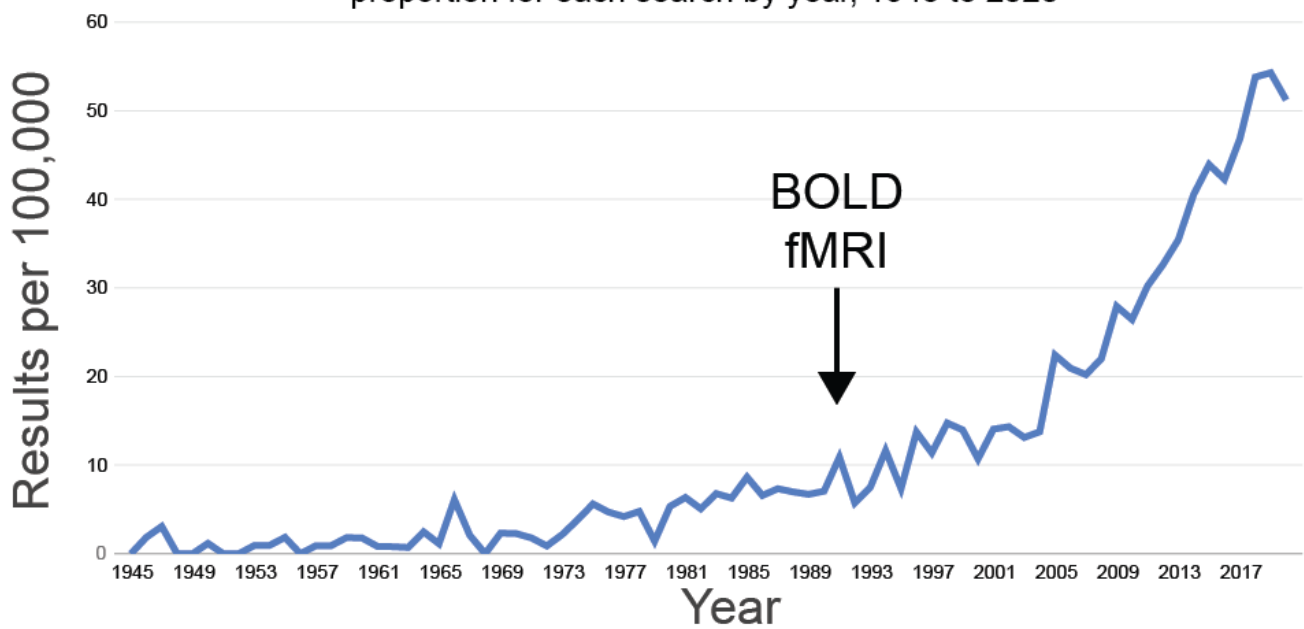### proportion for each search by year, 1945 to 2020

Fig. S8. The increase in publications related to brain atlases. | We searched for any publications since 1945 using the term "Brain Atlas" on PubMed. We note that since the introduction of BOLD fMRI in 1990, the need for neuroanatomical maps of the brain has increased, especially in the neuroimaging community. Many atlases have been published over the last 30 years, and many publications across the neuroscience literature have used these atlases. However, no comprehensive study exists evaluating, in any regard, to the suitability and nuances related to these atlases. We hope our work provides a valuable resource to others in our field, launches a larger discussion to critically evaluating the neuroanatomy of the brain, and direct future reproducible research for other scientists and clinician investigators.
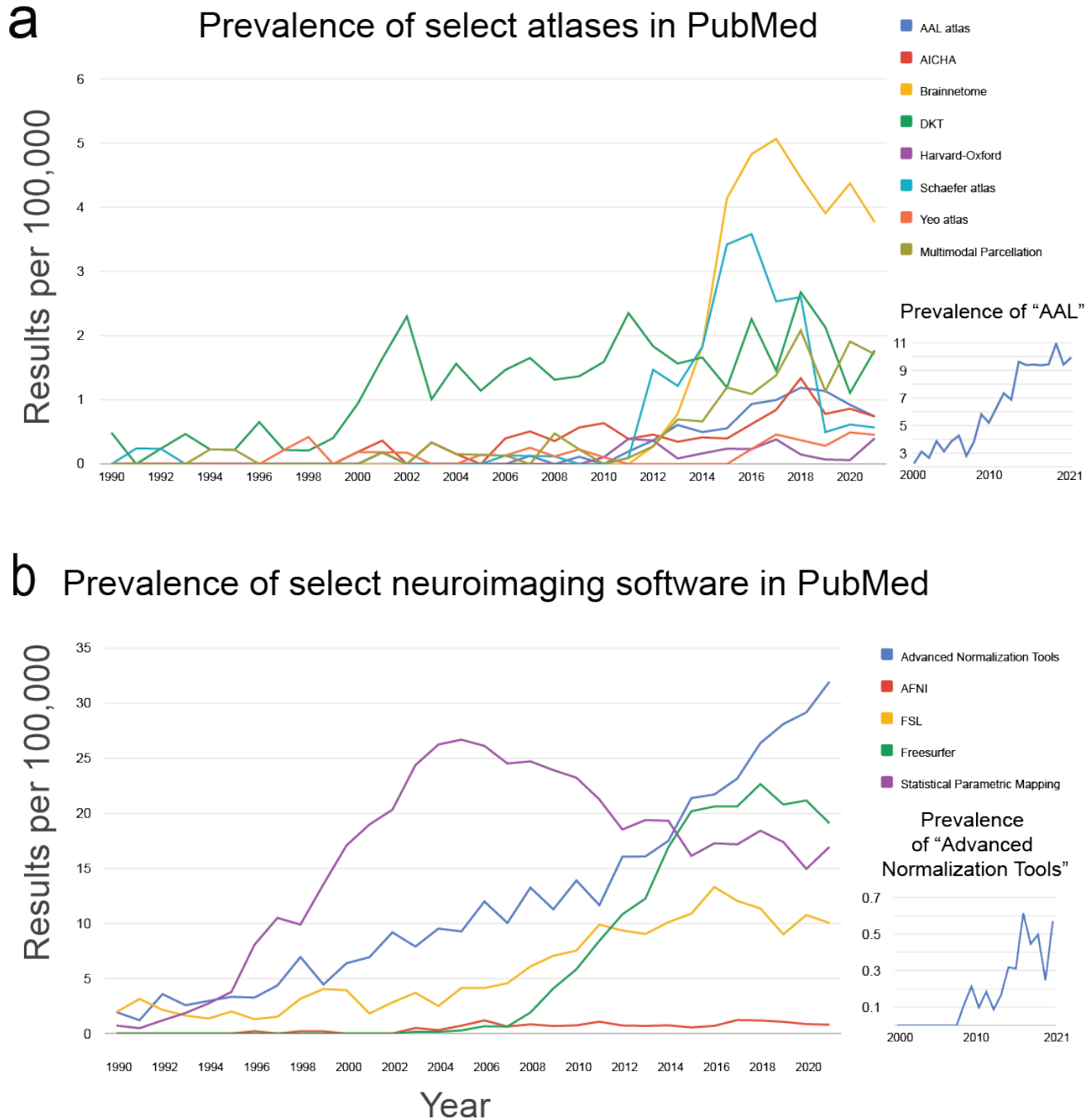
Fig. S9. Prevalence of select brain atlases and neuroimaging software | a, We searched on PubMed for any publications since 1945 using the verbatim terms shown in each line graph legend. The tool used is from https://esperr.github.io/pubmed-by-year/[89]. This search was done to gain a better understanding how often the field is using different tools, and thus to make some recommendations as to which atlases to use and facilitating the comparison of results. Note that due to the prevalence of the term "AAL" which may not relate to the AAL atlas, we opted for the term "AAL atlas". Another example is the use of "Multimodal Parcellation" rather than "MMP". The search for "AAL" is shown at the bottom right, where articles appear before the original AAL manuscript in 2002[88], most likely not relating to the AAL atlas. However, the prevalence of "AAL" increases substantially after 2002, more than other atlases. These search terms serves as a rough estimate of the prevalence of atlases, and may not reflect the true prevalence of each term. **b**, We show to prevalence of select neuroimaging software. Again, due to the ambiguity of search terms such as "ANTs", we opted for the full name of the software, despite some manuscripts only having used the abbreviated terms. "Advanced normalization tools" searched in quotes is shown at the bottom right, having first appeared formally in the literature in 2009[90].
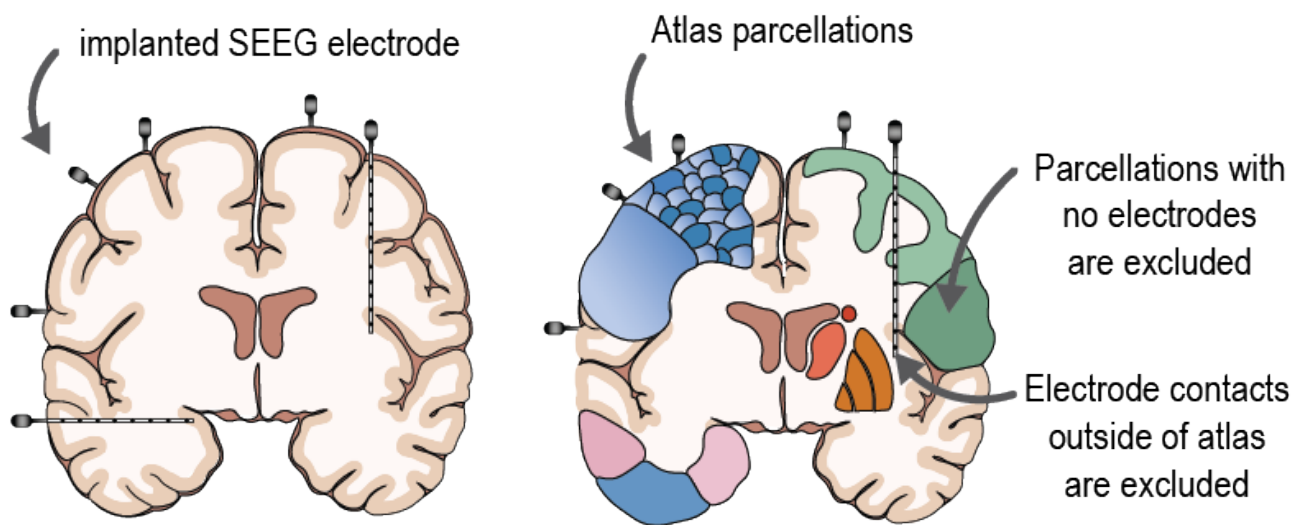
Fig. S10. Electrode localization and region selection | Assignment of each electrode contact to an atlas regions was performed by rounding electrode coordinates (x,y,z) to the nearest voxel and indexing the given atlas at that voxel. Electrodes that fell outside the atlas of interest were excluded from subsequent analysis. The structural connectivity network, representing normalized streamline counts between each atlas region, was also down sampled to only include regions that contained at least one SEEG contact. This gave one static representation of structural connectivity. In the case where multiple electrodes fell in the same atlas ROI, a random electrode was selected to represent the functional activity of that neuroanatomically defined region.

Patient	Age	Sex	Localization: suspected seizure onset zone		Control	Age	Sex
sub-patient01	58	M	Poorly localized. R temporal interictal activity.		sub-control01	24	M
sub-patient02	28	F	L anterior temporal lobe		sub-control02	40	F
sub-patient03	27	F	L hippocampus and amygdala		sub-control03	31	M
sub-patient04	20	F	L basal ganglia infarct		sub-control04	29	M
sub-patient05**	36	M	R frontal arteriovenous malformation		sub-control05	40	M
sub-patient06	57	F	Poorly localized. Possibly bitemporal onset		sub-control06	48	F
sub-patient07**	37	M	L temporal lobe/hippocampus/amygdala		sub-control07	22	M
sub-patient08**	34	M	R frontal, anterior cingulate gyrus		sub-control08	35	F
sub-patient09**	47	F	L hippocampus		sub-control09	27	F
sub-patient10	42	F	R temporal lobe/L temporal lobe		sub-control10	67	F
sub-patient11	27	M	L hippocampus, then amygdala		sub-control11	33	F
sub-patient12	35	M	Poorly localized. Possibly multifocal epilepsy		sub-control12	27	M
sub-patient13**	36	F	L temporal		sub-control13	NR	NR
sub-patient14**	29	F	L superior Frontal Sulcus				
sub-patient15	33	F	L mesial temporal lobe				
sub-patient16	29	M	Poorly localized. Possibly multifocal epilepsy				
sub-patient17	31	F	L mesial temporal lobe				
sub-patient18**	26	F	L heterotopia, left hippocampus				
sub-patient19**	23	M	L temporal/posterior lateral neocortical				
sub-patient20	30	M	L temporal encephalomalacia				
sub-patient21	24	M	R anterior temporal lobe				
sub-patient22	59	F	R frontal-parietal lobe				
sub-patient23	28	F	L or R superior temporal gyrus				
sub-patient24**	47	F	R anterior temporal				
sub-patient25	40	F	L temporal lobe near Heschl's gyrus				
sub-patient26	37	F	L amygdala/anterior temporal pole				
sub-patient27	30	M	L amygdala/hippocampus				
sub-patient28**	28	M	L mesial temporal lobe				

Table S2. Patient and control demographics. | Patient IDs with asterisk have clinically annotated seizures for structure-function calculation. Localization of the seizure onset zone was pulled from patient charts, either from the clinically hypothesized brain regions if the patient did not undergo surgery, or if the patient underwent surgery, the targeted location for resection or ablation. One control did not have age or sex information. **M**, Male; **F**: Female; **L**, left; **R**, Right; **NR**, Not reported